RIVISTA DEL NUOVO CIMENTO Vol. 36, N. 3 2013
DOI 10.1393/ncr/i2013-10086-y

Neutrino astronomy: An update

F. Halzen(*)
Department of Physics, University of Wisconsin - Madison, WI 53706, USA

ricevuto il 21 Novembre 2012

Summary. — Detecting neutrinos associated with the still enigmatic sources of cosmic rays has reached a new watershed with the completion of IceCube, the first detector with sensitivity to the anticipated fluxes. In this review, we will briefly revisit the rationale for constructing kilometer-scale neutrino detectors and summarize the status of the field.

PACS 95.85.Ry – Neutrino, muon, pion, and other elementary particles; cosmic rays.
PACS 98.70.Rz – γ-ray sources; γ-ray bursts.
PACS 98.70.Sa – Cosmic rays.

(*) E-mail: halzen@icecube.wisc.edu

1. – Introduction

Soon after the 1956 observation of the neutrino [1], the idea emerged that it represented the ideal astronomical messenger. Neutrinos reach us from the edge of the Universe without absorption and with no deflection by magnetic fields. Neutrinos have the potential to escape unscathed from the inner neighborhood of black holes and from, the subject of this update, the accelerators where cosmic rays are born. Their weak interactions also make cosmic neutrinos very difficult to detect. Immense particle detectors are required to collect cosmic neutrinos in statistically significant numbers [2]. Already by the 1970s, it had been understood that a kilometer-scale detector was needed to observe the "cosmogenic" neutrinos [3] (we will refer to them henceforth as BZ neutrinos) produced in the interactions of cosmic rays with background microwave photons [4].

Today's estimates of the sensitivity for observing potential cosmic accelerators such as Galactic supernova remnants, active galactic nuclei (AGN), and gamma-ray bursts (GRB) unfortunately point to the same exigent requirement [5]. Building a neutrino telescope has been a daunting technical challenge.

Given the detector's required size, early efforts concentrated on transforming large volumes of natural water into Cherenkov detectors that catch the light emitted by the secondary particles produced when neutrinos interact with nuclei in or near the detector [6]. After a two-decade-long effort, building the Deep Underwater Muon and Neutrino Detector (DUMAND) in the sea off the main island of Hawaii unfortunately failed [7]. However, DUMAND pioneered many of the detector technologies in use today and inspired the deployment of a smaller instrument in Lake Baikal [8] as well as efforts to commission neutrino telescopes in the Mediterranean [9-11]. These have paved the way toward the planned construction of KM3NeT.

The first telescope on the scale envisaged by the DUMAND collaboration was realized instead by transforming a large volume of deep, transparent, natural Antarctic ice into a particle detector, the Antarctic Muon and Neutrino Detector Array (AMANDA). In operation from 2000 to 2009, it represented the proof of concept for the kilometer-scale neutrino observatory, IceCube [12, 13].

Neutrino astronomy has already achieved spectacular successes: neutrino detectors have "seen" the Sun and detected a supernova in the Large Magellanic Cloud in 1987. Both observations were of tremendous importance; the former showed that neutrinos have a tiny mass, opening the first crack in the Standard Model of particle physics, and the latter confirmed the basic nuclear physics of the death of stars. Figure 1 illustrates the cosmic neutrino energy spectrum covering an enormous range, from the neutrinos produced in association with the 2.725 K microwave photon background to 10^{20} eV [14]. The figure is a mixture of observations and theoretical predictions. At low energy, the neutrino sky is dominated by neutrinos produced in the Big Bang. At MeV energy, neutrinos are produced by the Sun and by supernova explosions; the flux from the 1987 event is shown. At higher energies, the neutrino sky is dominated by neutrinos produced by cosmic-ray interactions in the atmosphere, measured up to energies of 100 TeV by the AMANDA experiment [15]. Atmospheric neutrinos are a key to our story, because they are the dominant background for extraterrestrial searches. The flux of atmospheric neutrinos falls dramatically with increasing energy; events above 100 TeV are rare, leaving a clear field of view of the sky for extraterrestrial sources.

Above a threshold of $\sim 4 \times 10^{19}$ eV, cosmic rays interact with the microwave background introducing an absorption feature in the cosmic-ray flux, the Greisen-Zatsepin-Kuzmin (GZK) cutoff. As a consequence, the mean free path of extragalactic cosmic

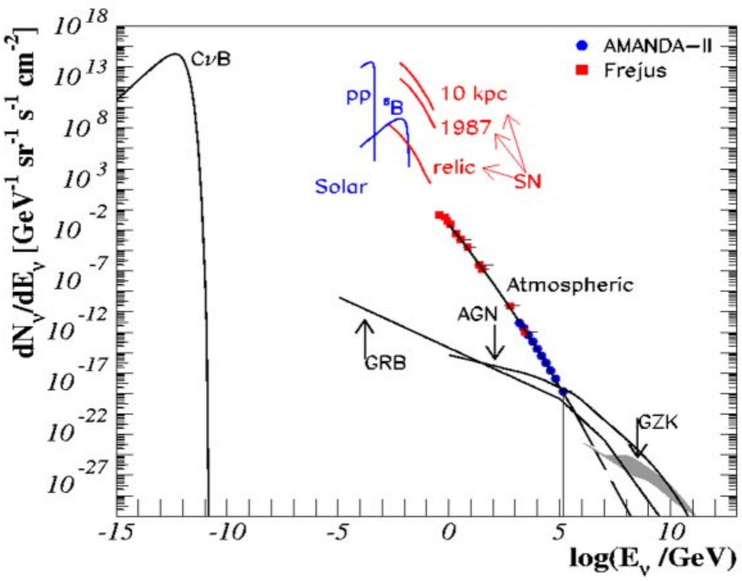

Fig. 1. – The cosmic-neutrino spectrum. Sources are the Big Bang (CνB), the Sun, supernovae (SN), atmospheric neutrinos, gamma-ray bursts (GRB), active galactic nuclei (AGN), and cosmogenic (GZK) neutrinos. The data points are from a detector at the Fréjus underground laboratory [17] (red) and from AMANDA [15] (blue). Figure courtesy of J. Becker [5].

rays propagating in the microwave background is limited to less than 100 megaparsecs. Therefore, the secondary neutrinos are the only probe of the still enigmatic sources at further distances. The highest energy neutrinos in fig. 1 are the decay products of pions produced by the interactions of cosmic rays with microwave photons [16]. The calculation of the neutrino flux associated with the observed flux of extragalactic cosmic rays is straightforward and yields on the order of one event per year in a kilometer-scale detector. The flux, labeled GZK in fig. 1, shares the high-energy neutrino sky with neutrinos anticipated from gamma-ray bursts and active galactic nuclei [5].

2. – Neutrino astronomy: methodology

The potential science of kilometer-scale neutrino detectors is rich, ranging from extreme astrophysics and the search for dark matter to the physics of the neutrinos themselves. The construction of neutrino telescopes is motivated by discovery. To maximize this potential, one must design an instrument with the largest possible effective telescope area to overcome the small neutrino cross-section with matter, and the best possible energy and angular resolution to address the wide diversity of possible signals. A major challenge is to separate any signal from the large background of cosmic-ray muons and atmospheric neutrinos of all flavors. On the other hand, these also provide a calibration beam to calibrate the novel instruments. While the smaller first-generation detectors have been optimized to detect secondary muons initiated by ν_μ, kilometer-scale neutrino observatories will detect neutrinos of all flavors over a wide range of energies.

We will review the methods by which we detect neutrinos, measure their energy and identify their flavor.

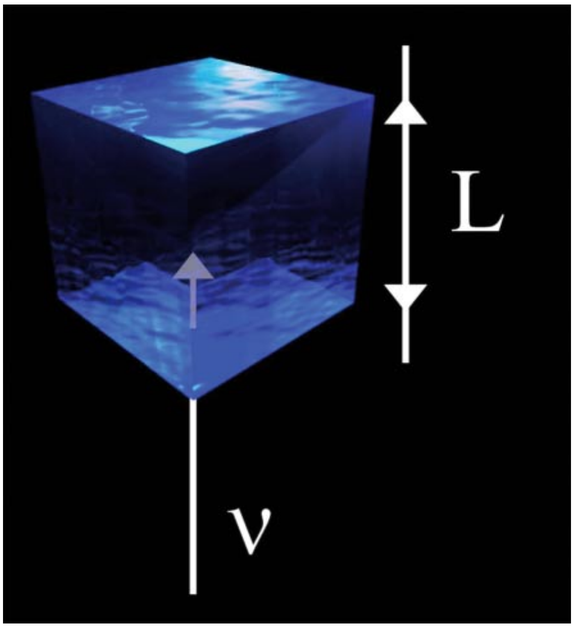

Fig. 2. – A neutrino interacts in a cube of instrumented ice of side L.

2·1. *Detection techniques*. – High-energy neutrinos are detected by observing the Cherenkov radiation from secondary particles produced in neutrino interactions inside large volumes of highly transparent ice or water instrumented with a lattice of photomultiplier tubes (PMT). For simplicity, assume an instrumented cubic volume of side L and a neutrino incident perpendicular to one side; see fig. 2. To a first approximation, a neutrino of energy E_ν incident on a side of area L^2 will be detected provided it interacts within the detector volume, *i.e.*, within the instrumented distance L. That probability is

$$P(E_\nu) = 1 - \exp[-L/\lambda_\nu(E_\nu)] \simeq L/\lambda_\nu(E_\nu), \tag{1}$$

where $\lambda_\nu(E_\nu) = [n\sigma_{\nu N}(E_\nu)]^{-1}$ is the neutrino mean free path. Here $\sigma_{\nu N}(E_\nu)$ is the neutrino-nucleon cross-section and $n = \rho_{\rm ice} N_A$ the target density, where $\rho_{\rm ice}$ is the density of the ice and N_A is Avogadro's number. A neutrino flux $\mathrm{d}N/\mathrm{d}E_\nu$, defined per unit area and unit time, crossing a detector with energy threshold $E_\nu^{\rm th}$ and cross-sectional area A $(= L^2)$ facing the incident beam will produce

$$N_{\rm ev} = T \int_{E_\nu^{\rm th}} A(E_\nu)\, P(E_\nu)\, \frac{\mathrm{d}N}{\mathrm{d}E_\nu}\, \mathrm{d}E_\nu \tag{2}$$

events after a time T. The formalism presented refers to an idealized detector; in practice, the "effective" detector area A is not strictly equal to the geometric cross-section of the instrumented volume facing the incoming neutrino because even neutrinos interacting outside the instrumented volume may produce a sufficient amount of light inside the detector to be detected. Also, not all of the events detected may be adequate for a particular scientific analysis. Therefore, A must be determined as a function of the incident neutrino direction by simulation of the full detector, including the trigger and the quality cuts on the data required for the specific analysis. Note that by substitution of eq. (1) into eq. (2) the integrand reduces to the volume of the detector multiplied by the target density and the neutrino cross-section and flux, a result that is physically evident.

This description applies to electron neutrinos; in the case of muon neutrinos, any neutrino producing a secondary muon that reaches the detector with sufficient energy to trigger it will be detected. Because the muon travels kilometers at TeV energies and tens of kilometers above PeV energy, muon neutrinos can be detected outside the instrumented volume; the probability is obtained by substitution in eq. (1) of

$$L \to \lambda_\mu, \tag{3}$$

which therefore yields

$$P = \lambda_\mu / \lambda_\nu. \tag{4}$$

Here, λ_μ is the range of the muon determined by its energy losses. Only "upgoing" neutrinos can be detected, the flux of "downgoing" secondary muons is overwhelmingly dominated by cosmic-ray muons. Up and down refer to the Northern and Southern Hemispheres in the case of IceCube. As we will see further on, there are methods to mitigate this problem and achieve complete sky coverage by measuring the energy of the events.

The flux of ν_μ-induced muons at the detector is given by a convolution of the neutrino spectrum $\mathrm{d}N/\mathrm{d}E_\nu$ with the probability P to produce a muon reaching the detector:

$$E_\mu \frac{\mathrm{d}N_\mu}{\mathrm{d}E_\mu}(E_\mu^{\min}, \theta) = \int_{E_\mu^{\min}} P(E_\nu, E_\mu^{\min}) \exp[-\sigma_{\mathrm{tot}}(E_\nu)\, N_A\, X(\theta)] \frac{\mathrm{d}N}{\mathrm{d}E_\nu}\, \mathrm{d}E_\mu, \tag{5}$$

where the secondary muon energy E_μ is related to the initial neutrino energy E_ν by $E_\mu = (1-y)\, E_\nu$. The additional exponential factor accounts for the absorption of neutrinos in the Earth along a chord of length $X(\theta)$ at zenith angle θ. Absorption becomes important for $\sigma_\nu(E_\nu) \gtrsim 10^{-33}\,\mathrm{cm}^2$ or $E_\nu \gtrsim 10^2\,\mathrm{TeV}$. The number of events is obtained by substituting eq. (4) and eq. (5) into eq. (2) and integrating over the energy of the secondary muons. For a detailed discussion, we refer the reader to [5] and the appendix of [18].

For back-of-the-envelope calculations, the P-function can be approximated by

$$P \simeq 1.3 \times 10^{-6} E^{2.2}, \quad \text{for } E = 10^{-3}\text{–}1\,\mathrm{TeV}, \tag{6}$$

$$\simeq 1.3 \times 10^{-6} E^{0.8}, \quad \text{for } E = 1\text{–}10^3\,\mathrm{TeV}. \tag{7}$$

At EeV energy(1), the increase is reduced to only $E^{0.4}$. Clearly, high-energy neutrinos are more likely to be detected because both the cross-section and muon range increase with energy.

(1) We will use energy units TeV, PeV and EeV, increasing by factors of 1000 from GeV energy.

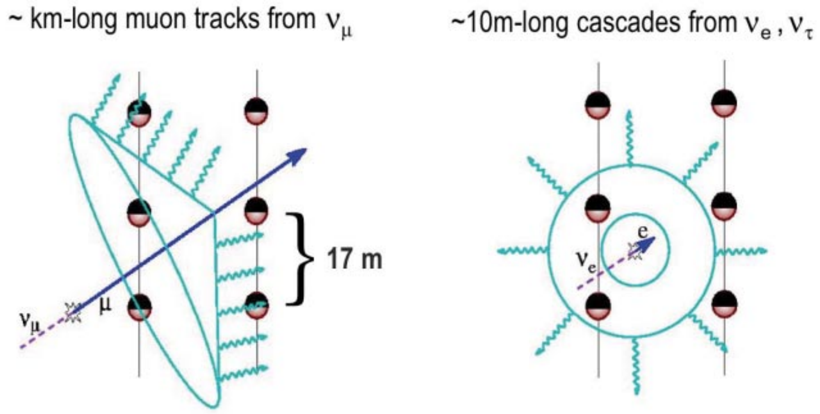

Fig. 3. – Contrasting Cherenkov light patterns produced by muons (left) and by secondary showers initiated by electron and tau neutrinos (right). Note that for IceCube the vertical distance between modules, 17 m, is shorter than the horizontal distance of 125 m. A muon with catastrophic energy loss will look like a superposition of the two panels.

Similar arguments apply to the detection of tau neutrinos. A tau neutrino will be detected provided the tau lepton it produces reaches the instrumented volume within its lifetime. Therefore, in eq. (1), L is replaced by

$$L \to \gamma c\tau = E/m\ c\tau, \tag{8}$$

where m, τ and E are the mass, lifetime and energy of the tau, respectively. The tau's decay length $\lambda_\tau = \gamma c\tau \approx 50\,\text{m} \times (E_\tau/10^3)\,\text{TeV}$ grows linearly with energy and actually exceeds the range of the muon near 1 EeV. The taus eventually range out by catastrophic interactions just like the muons, but this occurs at higher energy because the cross-sections are reduced by a factor of $(m_\mu/m_\tau)^2$.

The larger cross-sections of neutrinos, the longer range of the muon, and the longer lifetime of the tau at high energies make kilometer-scale neutrino detectors above a threshold of $\sim 100\,\text{GeV}$ possible. Because, at the energies of interest, the muon range and the decay length of a tau range from kilometers to tens of kilometers, muon and tau neutrinos can be detected over volumes of ice and water larger than the actual instrumented volume.

2·2. *Identification of neutrino flavors*. – Although we have concentrated so far on the secondary leptons that carry most of the neutrino energy, in a Cherenkov detector, the light of the secondary showers is detected as well as the light produced by showers initiated by neutral current interactions of neutrinos of all flavors. Because the size of showers, on the order of 10 m in ice at the energies of interest, is small compared to the spacing of the PMTs, they represent, to a good approximation, a point source of Cherenkov photons radiated by the shower particles. These trigger the PMTs at the single photoelectron level over a spherical volume whose radius scales linearly with the shower energy; see fig. 3. In the absence of a track, the reconstruction of the neutrino arrival direction is more challenging.

Whereas the smaller first-generation telescopes mostly exploit the large range of the muon to increase their effective area for ν_μ, kilometer-scale detectors can fully exploit the advantages associated with the detection of showers initiated by ν_e and ν_τ:

1) Neutrinos are detected over both the Northern and Southern Hemispheres. We should note that this is also the case for ν_μ with energy in excess of 1 PeV where the background from the steeply falling atmospheric spectrum is negligible.

2) The background of atmospheric neutrinos is significantly reduced. At high energies the muons from π decay, the source of atmospheric ν_e, no longer decay, and relatively rare K-decays become the dominant source of background electron neutrinos.

3) Energy measurement is superior. The detector is a complete absorption calorimeter; this is not the case for muon neutrinos where it only samples the energy loss of the muon inside the detector.

4) Tau neutrinos are not absorbed by the Earth.

The generic cosmic accelerator produces neutrinos from the decay of pions with a flavor admixture of $\nu_e : \nu_\mu : \nu_\tau = 1 : 2 : 0$. This is also the composition of the atmospheric neutrino beam below 10 GeV energy where the muons decay. Because of neutrino oscillations, the ratio detected is modified to 1 : 1 : 1 as approximately one half of the muon neutrinos reappear with tau flavor over large baselines. This represents an advantage because ν_τ, unlike ν_e and ν_μ, are not absorbed in the Earth. The reason is simple [19]. A ν_τ interacting in the Earth will produce a secondary ν_τ of lower energy, either directly in a neutral current interaction or via the decay of a tau lepton produced in a charged current interaction. High-energy ν_τ will thus cascade down to ~ 70 TeV energy where the Earth is transparent. In other words, although detected with a reduced energy, they are not absorbed.

2·2.1. Electron neutrinos. High-energy electron neutrinos deposit 80% of their energy in an electromagnetic shower initiated by the secondary electron. The rest of the energy goes into the fragments of the target that produce a second subdominant shower. For ice, the Cherenkov light generated by shower particles spreads over a volume of radius 130 m at 10 TeV and 460 m at 10 EeV in the top half of the IceCube detector (180 m and 540 m in the bottom half where the absorption length is increased) [20]; *i.e.*, the shower radius grows by 55 m (60 m) per decade in energy.

The measurement of the radius of the lightpool mapped by the lattice of PMTs determines the energy and turns neutrino telescopes into total absorption calorimeters [12]. Note that a contained event of 10 EeV neutrino energy will not fill a km^3 detector volume. So, even for a BZ neutrino, the energy of the event can be measured.

Because the shower and its accompanying Cherenkov lightpool are not totally symmetric but elongated in the direction of the leading electron, the direction of the incident neutrino can be reconstructed. Pointing is however inferior to what can be achieved for muon neutrinos and is estimated to be precise to the order of only 10 degrees [12]. We will revisit this subject in more detail when we review IceCube observations further on.

2·2.2. Muon neutrinos. Secondary muons initiated by muon neutrinos with energy in excess of ~ 1 TeV generate showers along their track by bremsstrahlung, pair production, and photonuclear interactions. These are the sources of additional Cherenkov radiation. In the first kilometer, a high-energy muon typically loses energy in a couple of showers of one tenth its initial energy. Note however that, unlike for showers, the energy measurement is indirect. Because of the stochastic nature of muon energy loss, the logarithm of the energy is measured. Also, although at PeV energy and above muons have a range of tens of kilometers, greatly enhancing their detectability, the initial energy of the event can only be inferred. A muon can be produced at one energy, travel several kilometers, and be detected with much less energy.

2·2.3. Tau neutrinos. Tau flavor is a powerful signature of cosmic origin because the production of high-energy ν_τ in the atmosphere is suppressed by some five orders of magnitude relative to ν_e and ν_μ; at high energies a ν_τ is a cosmic neutrino. Whereas at lower energies ν_τ produce showers difficult to distinguish from those initiated by ν_e, the flavor of tau neutrinos of sufficiently high energy can be identified. Perhaps the most striking signature is the double-bang event [21] in which the production and decay of a τ lepton are detected as two separated showers inside the detector. However, the probability of detecting and identifying a ν_τ as a double-bang is only 10% of that for detecting a ν_μ of the same energy in the 10 PeV energy range. At lower and higher energies, the likelihood of detecting a double-bang falls rapidly. It may also be possible to identify events in which a ν_τ creates a minimum-ionizing track of length $30\,\mathrm{m} \times E_{\mathrm{PeV}}$ that penetrates the detector and ends in a high-energy cascade when the τ lepton decays. The parent τ track can be identified by the reduced catastrophic energy loss compared to a muon of similar energy. For more detailed discussions on tau neutrino detection, see [12] and [22].

2·3. *The first kilometer-scale neutrino detector: IceCube.* – A series of first-generation experiments [23, 24] have demonstrated that high-energy neutrinos with $\sim 10\,\mathrm{GeV}$ energy and above can be detected using large volumes of highly transparent ice or water instrumented with a lattice of photomultiplier tubes. Such instruments detect neutrinos by observing Cherenkov radiation from secondary particles produced in neutrino interactions inside the detector. Construction of the first second-generation detector, IceCube, at the geographic South Pole was completed in December 2010 [25]; see fig. 4.

IceCube consists of 80 strings, each instrumented with 60 ten-inch photomultipliers spaced 17 m apart over a total length of one kilometer. The deepest modules are located at a depth of 2.45 km so that the instrument is shielded from the large background of cosmic rays at the surface by approximately 1.5 km of ice. Strings are arranged at apexes of equilateral triangles that are 125 m on a side. The instrumented detector volume is a cubic kilometer of dark and highly transparent [26] Antarctic ice. The ice is sterile with the radioactive background dominated by the instrumentation deployed in this natural ice.

Each optical sensor consists of a glass sphere containing the photomultiplier and the electronics board that digitizes the signals locally using an onboard computer. The digitized signals are given a global time stamp with residuals accurate to less than 3 ns and are subsequently transmitted to the surface. Processors at the surface continuously collect the time-stamped signals from the optical modules, each of which functions independently. The digital messages are sent to a string processor and a global event builder. They are subsequently sorted into the Cherenkov patterns emitted by secondary muon tracks, or electron and tau showers, that reveal the direction of the parent neutrino; see [20].

Based on data taken during construction, the actual effective area of the completed IceCube detector is larger by a factor 2 (3) at PeV (EeV) energy over what had been

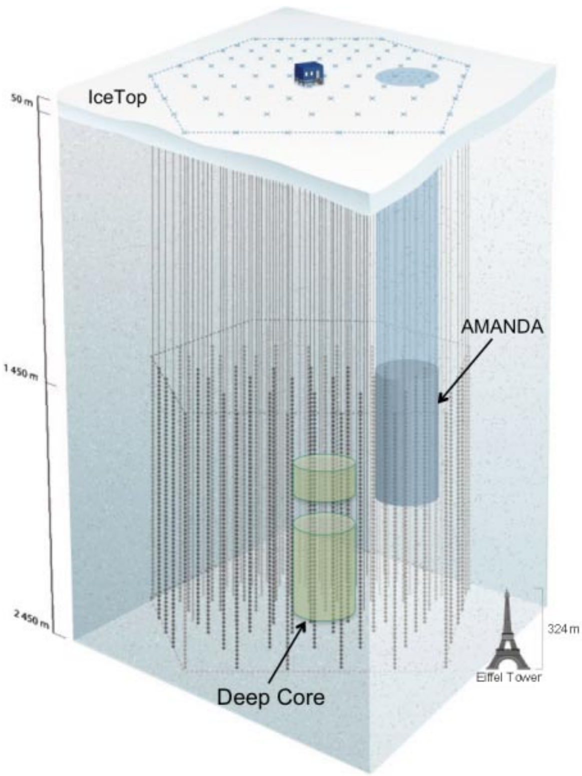

Fig. 4. – Schematic of the IceCube detector.

expected [13], mostly because of improvements to the data acquisition system. The neutrino-collecting area is expected to increase further with improved calibration and development of optimized software tools for the detector, which has been operating stably in its final configuration since May 2011. Already reaching an angular resolution of better than 0.5 degree for muon tracks triggered, this resolution can be reduced off-line to ≤ 0.2 degree for individual events. The absolute pointing has been determined by measuring the shadowing of cosmic-ray muons by the moon to 0.1 degree at FWHM.

IceCube detects 10^{11} muons per year at a trigger rate of 2700 Hz. Among these it filters 10^5 neutrinos, one every six minutes, above a threshold of ~ 100 GeV. The DeepCore infill array (fig. 4) identifies a sample, roughly equal in number depending on the quality cuts, with energies as low as 10 GeV; see fig. 5. These muons and neutrinos are overwhelmingly of atmospheric origin and are the decay products of pions and kaons produced by collisions of cosmic-ray particles with nitrogen and oxygen nuclei in the atmosphere. With larger detectors, the separation of cosmic-ray muons from secondary muons of neutrino origin becomes relatively straightforward even though their ratio is at the level of $10^6 : 1$. Muons tracks are reconstructed by likelihood methods and their energy deposition in the detector is determined in real time. High-purity neutrino samples of upgoing muon tracks of neutrino origin are separated from downgoing cosmic-ray muons by quality cuts; for instance, on the likelihood of the fit, on the number of photons that arrive at DOMs at the Cherenkov time (*i.e.*, without a significant time delay

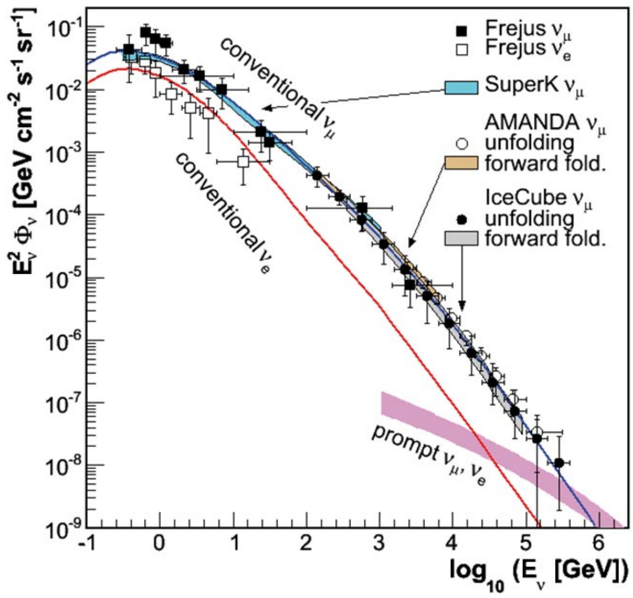

Fig. 5. – Measurements of the atmospheric neutrino energy spectrum; from Fréjus [27], SuperK [28], AMANDA forward-folding [29] and unfolding analyses [30], and IceCube (40 strings) forward-folding [31] and unfolding analyses [32]. All measurements include the sum of neutrinos and antineutrinos. The expectations for the conventional ν_μ and ν_e flux are from [33]. The prediction for the prompt flux is from [34].

resulting from scattering), on the length of the track, on the "smoothness" requiring a uniform distribution of photoelectrons along the length of the track, etc. Each analysis produces appropriate cuts depending on the magnitude of the background and the purity required to isolate an eventual signal.

Atmospheric neutrinos are a background for cosmic neutrinos, at least at energies below 100 TeV where the flux becomes too small to produce events in a kilometer-scale detector; see fig. 5. At the highest energies, a small charm component is anticipated; its magnitude is uncertain and remains to be measured. As in conventional astronomy, IceCube must look through the atmosphere for cosmic neutrinos.

3. – Two cosmic-ray puzzles

Despite their discovery potential touching a wide range of scientific issues, the construction of ground-based gamma-ray telescopes and kilometer-scale neutrino detectors has been largely motivated by the possibility of opening a new window on the Universe in the TeV energy region, and above in the case of neutrinos. In this review, we will revisit the prospects for detecting gamma rays and neutrinos associated with cosmic rays, thus revealing their sources at a time when we are commemorating the 100th anniversary of their discovery by Victor Hess in 1912.

Cosmic accelerators produce particles with energies in excess of 10^8 TeV; we still do not know where or how [35]. The flux of cosmic rays observed at Earth is shown in fig. 6. The energy spectrum follows a sequence of three power laws. The first two are separated

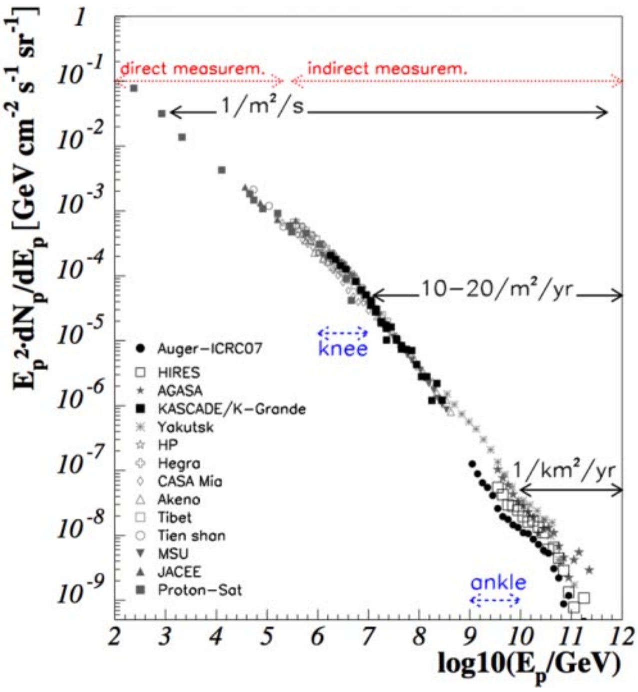

Fig. 6. – At the energies of interest here, the cosmic-ray spectrum follows a sequence of three power laws. The first two are separated by the "knee," and the second and third by the "ankle." Cosmic rays beyond the ankle are a new population of particles produced in extragalactic sources. Figure from J. Becker [5].

by a feature dubbed the "knee" at an energy of approximately 3 EeV. There is evidence that cosmic rays up to this energy are Galactic in origin.

Any association with our Galaxy disappears in the vicinity of a second feature in the spectrum referred to as the "ankle"; see fig. 6. Above the ankle, the gyroradius of a proton in the Galactic magnetic field exceeds the size of the Galaxy, and we are almost certainly witnessing the onset of an extragalactic component in the spectrum that extends to energies beyond 100 EeV. Support for this assumption now comes from three experiments [36] that have observed the telltale structure in the cosmic-ray spectrum resulting from the absorption of the particle flux by the microwave background, the GZK cutoff. Neutrinos are produced in GZK interactions; it was already recognized in the 1970s that their observation requires kilometer-scale neutrino detectors. The origin of the cosmic-ray flux in the intermediate region covering PeV-to-EeV energies remains a mystery, although it is routinely assumed that its origin is some mechanism extending the reach of Galactic accelerators.

Acceleration of protons (or nuclei) to TeV energy and above requires massive bulk flows of relativistic charged particles. These are likely to originate from exceptional gravitational forces in the vicinity of black holes or neutron stars. The gravity of the collapsed objects powers large currents of charged particles that are the origin of high magnetic fields. These create the opportunity for particle acceleration by shocks. It is a fact that electrons are accelerated to high energy near black holes; astronomers detect them indirectly by their synchrotron radiation. Some cosmic sources must accelerate protons, because we observe them as cosmic rays.

The detailed blueprint for a cosmic-ray accelerator must meet two challenges: the highest energy particles in the beam must reach beyond 10^3 TeV (10^8 TeV) for Galactic (extragalactic) sources, and their luminosities must be able to accommodate the observed cosmic-ray flux. Both represent severe constraints that have limited theoretical speculations.

Supernova remnants were proposed as possible sources of Galactic cosmic rays as early as 1934 by Baade and Zwicky [37]; their proposal is still a matter of debate after more than 75 years [38]. Galactic cosmic rays reach energies of at least several PeV, the "knee" in the spectrum. Their interactions with Galactic hydrogen in the vicinity of the accelerator should generate gamma rays from the decay of secondary pions that reach energies of hundreds of TeV. Such sources should be identifiable by a relatively flat energy spectrum that extends to hundreds of TeV without attenuation; they have been dubbed PeVatrons. The search to pinpoint them has so far been unsuccessful.

Although there is no incontrovertible evidence that supernovae accelerate cosmic rays, the idea is generally accepted because of energetics: three Galactic supernova explosions per century converting a reasonable fraction of a solar mass into particle acceleration can accommodate the steady flux of cosmic rays in the Galaxy. Energetics also drives speculations on the origin of extragalactic cosmic rays.

By integrating the cosmic-ray spectrum in fig. 6 above the ankle, we find that the energy density of the Universe in extragalactic cosmic rays is $\sim 3\times10^{-19}\,\mathrm{erg\,cm^{-3}}$ [39]. This value is rather uncertain because of our ignorance of the precise energy where the transition from Galactic to extragalactic sources occurs. The power required for a population of sources to generate this energy density over the Hubble time of 10^{10} years is $2\times10^{37}\,\mathrm{erg\,s^{-1}}$ per $\mathrm{Mpc^3}$ (in the astroparticle community, this flux is also known as $5\times10^{44}\,\mathrm{TeV\,Mpc^{-3}\,yr^{-1}}$). A gamma-ray-burst fireball converts a fraction of a solar mass into the acceleration of electrons, seen as synchrotron photons. The observed energy in extragalactic cosmic rays can be accommodated with the reasonable assumption that shocks in the expanding GRB fireball convert roughly equal energy into the acceleration of electrons and cosmic rays [40]. It so happens that 2×10^{51} erg per GRB will yield the observed energy density in cosmic rays after 10^{10} years, given that their rate is on the order of 300 per $\mathrm{Gpc^3}$ per year. Hundreds of bursts per year over Hubble time produce the observed cosmic-ray density, just like three supernovae per century accommodate the steady flux in the Galaxy.

Problem solved? Not really: it turns out that the same result can be achieved assuming that active galactic nuclei convert, on average, $2\times10^{44}\,\mathrm{erg\,s^{-1}}$ each into particle acceleration [5]. As is the case for GRBs, this is an amount that matches their output in electromagnetic radiation. Whether GRBs or AGN, the observation that these sources are required to radiate similar energies in photons and cosmic rays is unlikely to be an accident. We discuss the connection next; it will lead to a prediction of the neutrino flux.

4. – Neutrinos (and photons) associated with cosmic rays

How many gamma rays and neutrinos are produced in association with the cosmic-ray beam? Generically, a cosmic-ray source should also be a neutrino-producing beam dump. Cosmic rays accelerated in regions of high magnetic fields near black holes inevitably interact with radiation surrounding them. These may be photons radiated by the accretion disk in AGN or synchrotron photons that co-exist with protons in the exploding fireball producing a GRB. In these interactions, neutral and charged pion secondaries are produced by the processes

$$p + \gamma \to \Delta^+ \to \pi^0 + p \qquad \text{and} \qquad p + \gamma \to \Delta^+ \to \pi^+ + n. \tag{9}$$

While secondary protons may remain trapped in the high magnetic fields, neutrons and the decay products of neutral and charged pions escape. The energy escaping the source is therefore distributed among cosmic rays, gamma rays and neutrinos produced by the decay of neutrons, neutral pions and charged pions, respectively.

In the case of Galactic supernova shocks, cosmic rays inevitably interact with the hydrogen in the Galactic disk, producing equal numbers of pions of all three charges in hadronic collisions $p + p \to N\,[\pi^0 + \pi^+ + \pi^-] + X$; N is the pion multiplicity. Their secondary fluxes should be boosted by the interaction of the cosmic rays with high-density molecular clouds that are ubiquitous in the star-forming regions where supernovae are more likely to explode.

In a generic cosmic beam dump, accelerated cosmic rays, assumed to be protons for simplicity, interact with a photon or proton target. In either case, accelerated cosmic rays produce charged and neutral pions. Subsequently, the pions decay into gamma rays and neutrinos that carry, on average, 1/2 and 1/4 of the energy of the parent pion. We here assume that the four leptons in the decay $\pi^+ \to \nu_\mu + \mu^+ \to \nu_\mu + (e^+ + \nu_e + \bar{\nu}_\mu)$ equally share the charged pion's energy. The energy of the pionic leptons relative to the proton is

$$x_\nu = \frac{E_\nu}{E_p} = \frac{1}{4}\langle x_{p\to\pi}\rangle \simeq \frac{1}{20} \tag{10}$$

and

$$x_\gamma = \frac{E_\gamma}{E_p} = \frac{1}{2}\langle x_{p\to\pi}\rangle \simeq \frac{1}{10}\,. \tag{11}$$

Here

$$\langle x_{p\to\pi}\rangle = \left\langle \frac{E_\pi}{E_p} \right\rangle \simeq 0.2 \tag{12}$$

is the average energy transferred from the proton to the pion.

5. – Sources of the extragalactic cosmic rays

Waxman and Bahcall [41] have presented an interesting benchmark for the neutrino flux expected from extragalactic cosmic ray accelerators, whatever they may be. Assuming an E^{-2} spectrum of the accelerators, the cosmic-ray flux can be parametrized as

$$\frac{\mathrm{d}N_p}{\mathrm{d}E_p} = \frac{5\times 10^{-11}}{E_p^2}\,\mathrm{TeV}^{-1}\,\mathrm{cm}^{-2}\,\mathrm{s}^{-1}\,\mathrm{sr}^{-1}. \tag{13}$$

Integrating this flux, from the ankle to a maximal accelerator energy of 10^9 TeV, accommodates the total energy requirement of $\sim 3\times 10^{-19}\,\mathrm{erg\,cm}^{-3}$. Injecting this flux in the microwave background leads to a spectrum that agrees with the observed flux. The secondary neutrino flux is given by [42]

$$\frac{\mathrm{d}N_\nu}{\mathrm{d}E_\nu} = \frac{1}{3}\left[\frac{2}{3}\right]\frac{1}{x_\nu}\frac{\mathrm{d}N_p}{\mathrm{d}E_p}\left(\frac{E_\nu}{x_\nu}\right). \tag{14}$$

Here the coefficients 1/3 and 2/3 correspond to photo- and hadroproduction of the neutrinos, respectively. $N_\nu (= N_{\nu_\mu} = N_{\nu_e} = N_{\nu_\tau})$ represents the sum of the neutrino and antineutrino fluxes which are not distinguished by the experiments. Oscillations over cosmic baselines yield approximately equal fluxes for the three flavors. For the cosmic-ray flux introduced above, we obtain a neutrino flux

$$\frac{\mathrm{d}N_\nu}{\mathrm{d}E_\nu} \simeq \frac{2\times 10^{-12}}{E_p^2}\,\mathrm{TeV}^{-1}\,\mathrm{cm}^{-2}\,\mathrm{s}^{-1}\,\mathrm{sr}^{-1}. \tag{15}$$

Notice that we sneaked in the assumption that each cosmic ray interacts once and only once in the target —if not, the flux is multiplied by the number of interactions n_{int}; see [42] for a detailed discussion. In fact, Waxman and Bahcall have argued that, if the density of the source were such that a high-energy cosmic ray interacted more than once, it would be opaque to TeV photons. So, the neutrino flux represents an upper limit for extragalactic sources that emit TeV gamma rays.

5˙1. *Gamma ray bursts.* – It is important to realize that the high-energy protons may be magnetically confined to the accelerator. In the case of GRBs, for instance, protons adiabatically lose energy, trapped inside the fireball that expands under radiation pressure until it becomes transparent and produces the display observed by astronomers. Secondary neutrons do escape with high energies and decay into protons that are the source of the observed extragalactic cosmic-ray flux [43]. In this case, cosmic rays and pionic neutrinos are directly related by the fact that, for each secondary neutron decaying into a cosmic-ray proton, there are three neutrinos produced by the associated π^+ (see eq. (9)):

$$E_\nu\frac{\mathrm{d}N_\nu}{\mathrm{d}E_\nu} = 3\;E_n\,\frac{\mathrm{d}N_n}{\mathrm{d}E_n}(E_n) \tag{16}$$

and, after oscillations

$$E_\nu^2\frac{\mathrm{d}N_\nu}{\mathrm{d}E_\nu} \simeq \left(\frac{x_\nu}{x_n}\right)E_n^2\,\frac{\mathrm{d}N_n}{\mathrm{d}E_n}(E_n) \tag{17}$$

per neutrino flavor, where $x_n \sim 1/2$ is the relative energy of the secondary neutron; the neutron flux is identified with the observed cosmic-ray flux. This straightforward prediction has been ruled out by IceCube with data taken during construction [44]. There are alternative scenarios, including the one originally proposed by Waxman and Bahcall [45], that, fortunately, also yield predictions within reach of the completed detector within several years.

The key feature is that the normalization of the generic neutrino flux of eq. (14) is correct for GRBs because the fireball model generically predicts that $n_{\mathrm{int}} \simeq 1$. The GRB phenomenology that successfully accommodates the astronomical observations, as well

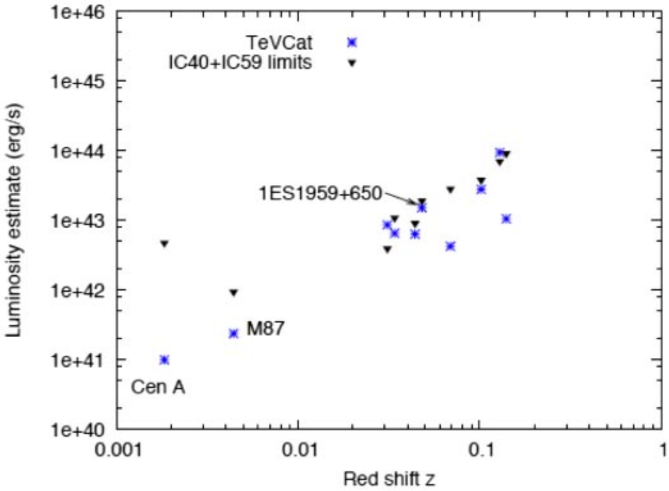

Fig. 7. – Limits on the neutrino flux from selected active galaxies derived from IceCube data when the instrument was operating during construction with 40 and 59 strings out of 86 instrumented strings of DOMs. These are compared with the TeV photon flux for nearby AGN. Note that energy units are in erg, not TeV. Figure courtesy of T. Gaisser.

as the acceleration of cosmic rays, is that of the creation of a hot fireball of electrons, photons and protons that is initially opaque to radiation. The hot plasma therefore expands by radiation pressure, and particles are accelerated to a Lorentz factor Γ that grows until the plasma becomes optically thin and produces the GRB display. The rapid time structure of the burst is associated with successive shocks (shells), of width $\Delta R = c \times t_v$, that develop in the expanding fireball. The rapid temporal variation of the radiation, t_v, is on the order of milliseconds, and can be interpreted as the collision of internal shocks with different Lorentz factors. Electrons, accelerated by first-order Fermi acceleration, radiate synchrotron gamma rays in the strong internal magnetic field, and thus produce the spikes observed in the emission spectra. The number of interactions of protons with the synchrotron photons is simply determined by the optical depth of the fireball shells of width ΔR to $\mathrm{p}\,\gamma$ interactions and is generically on the order of $n_{\mathrm{int}} \simeq 1$.

5·2. *Active galaxies*. – No compelling prediction is possible for AGN, complex systems with many possible sites for acceleration and interaction of the cosmic rays. Our discussion has, however, introduced the rationale that generic cosmic-ray sources produce a neutrino flux comparable to their flux of cosmic rays [39] and pionic TeV gamma rays [46]. In this context, we introduce fig. 7, which shows the present IceCube upper limits on the neutrino flux from nearby AGN as a function of their distance. Also shown is the TeV gamma-ray emission from the same sources. Except for CenA and M87, the muon-neutrino limits have reached the level of the TeV photon flux. This is a notable fact because of the roughly equal sharing of the cosmic-ray, gamma-ray and neutrino fluxes from a cosmic-ray accelerator. One can sum the sources shown in the figure into a diffuse flux; the result is, after dividing by $4\pi/c$ to convert the point source to a diffuse flux, $3 \times 10^{-12}\,\mathrm{TeV\,cm^{-2}\,s^{-1}\,sr^{-1}}$, or approximately $10^{-11}\,\mathrm{TeV\,cm^{-2}\,s^{-1}\,sr^{-1}}$ for all neutrino flavors. This flux matches the "maximal" flux previously argued for; see fig. 8.

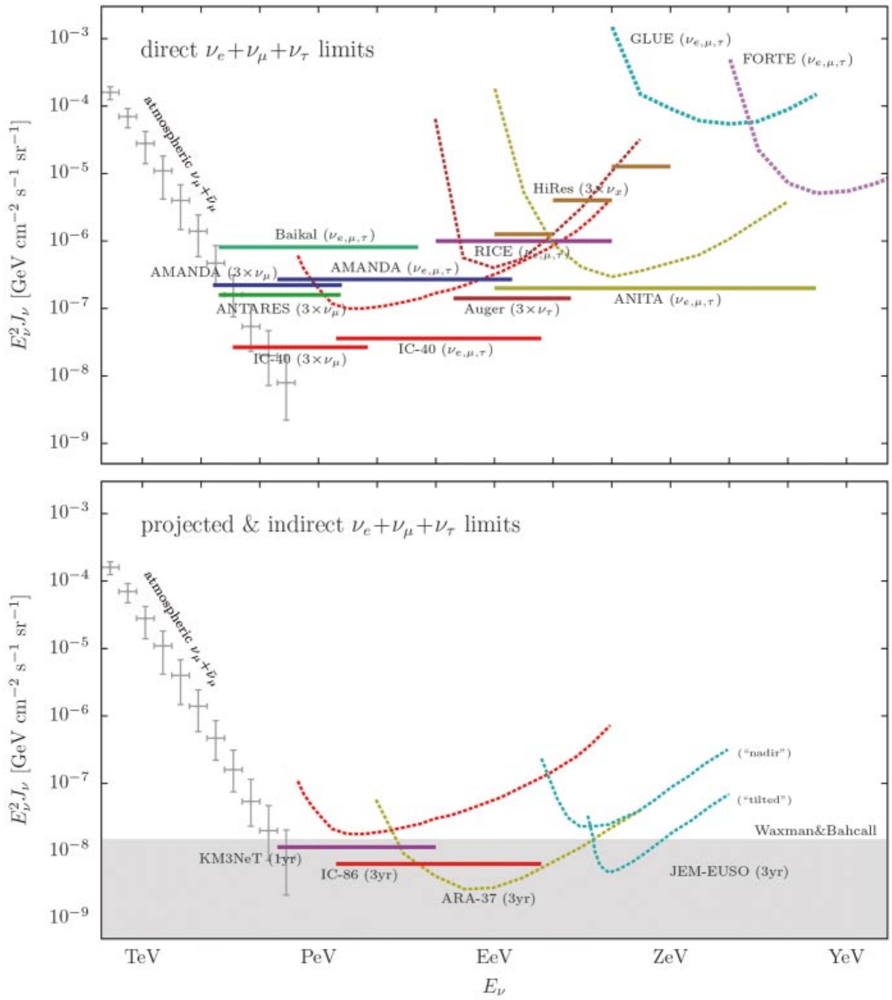

Fig. 8. – Limits on a diffuse neutrino flux from existing (top) and future (bottom) experiments; see [48]. The quantity on the vertical axis is referred to as $E_\nu^2 \mathrm{d}N_\nu/\mathrm{d}E_\nu$ in the text and is in GeV units here. The shaded band indicates the anticipated neutrino fluxes associated with cosmic rays. Figure courtesy of M. Ahlers.

IceCube's sensitivity is rapidly approaching this benchmark flux as shown in fig. 8. In fact, the latest IceCube "limit" recently obtained with one year of data taken with 59 strings is a 1.8σ flux [47]. A 2.3σ high-energy excess, instead of a limit, has also been identified in a measurement of the diffuse flux of shower events based on data from the 40-string detector. Although not significant, it is of interest that the benchmark flux argued for lies above the atmospheric neutrino background in fig. 8 for energies exceeding 100 TeV, a flux level already reached by the completed IceCube detector after one year of operation.

5·3. *Neutrinos from GZK interactions*. – The improved performance of IceCube at EeV energy has created the opportunity to detect neutrinos from GZK interactions.

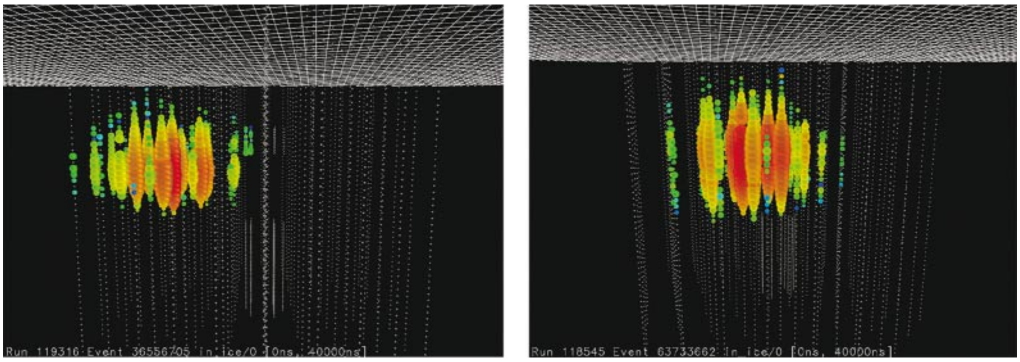

Fig. 9. – Displays of the two observed events. Each colored sphere represents a DOM that sent a time-stamped waveform to the event builder. Colors indicate the arrival time of the photon (red=early, blue=late). The size of the sphere indicates the number of photons detected by each DOM.

We anticipate 2.3 events in three years of running the completed detector assuming a flux derived from the "best fit" to the cosmic-ray data [16], and 4.8 events for the largest neutrino rate allowed by the constraint that the accompanying electromagnetic flux resulting from the production of neutral pions not exceed the known flux of diffuse photons in the Universe [16].

Throughout the discussion of the neutrino flux associated with extragalactic cosmic rays we have neglected the fact that neutrinos, unlike cosmic rays, are not absorbed by microwave photons, resulting in a neutrino flux not attenuated by "a factor" that depends on the cosmological evolution of the sources with redshift. We have also assumed that the highest energy cosmic rays are protons. Experiments disagree on the composition but the cosmogenic neutrino flux is inevitably reduced in the case of heavy primaries.

Recently, in a dedicated search for cosmogenic neutrinos, two events have been found [49] in the first year of data taken with the completed detector. They are contained showers more than 500 m in size that start inside the detector and produce about 10^5 photoelectrons. With no evidence of a muon track, they are initiated by electron or tau neutrinos; see fig. 9. However, their energies, rather than super-EeV as expected for cosmogenic neutrinos, are in the PeV range: 1.1 and 1.3 PeV with a negligible statistical error and a 35% systematic error. The analysis of these events is ongoing and we expect this error to be significantly reduced in the near future.

We are in the process of determining the directions of the initial neutrinos, exploiting the fact that the waveforms collected by the DOMs following and trailing the initial neutrino direction are identifiably different [12]; see fig. 10.

More importantly, we have designed a dedicated analysis to find more such starting events in the same data sample. Some of them should contain muon tracks whose arrival directions can be reconstructed with superior precision to that of the two shower events. The events represent an interesting hint for new neutrino physics, or astrophysics, because their origin as conventional atmospheric neutrinos is excluded at the 2.9σ level [49]. Accommodating the events as the decay of charm particles produced in the atmosphere would require a flux that violates the IceCube diffuse limit obtained with data collected with 59 strings [47].

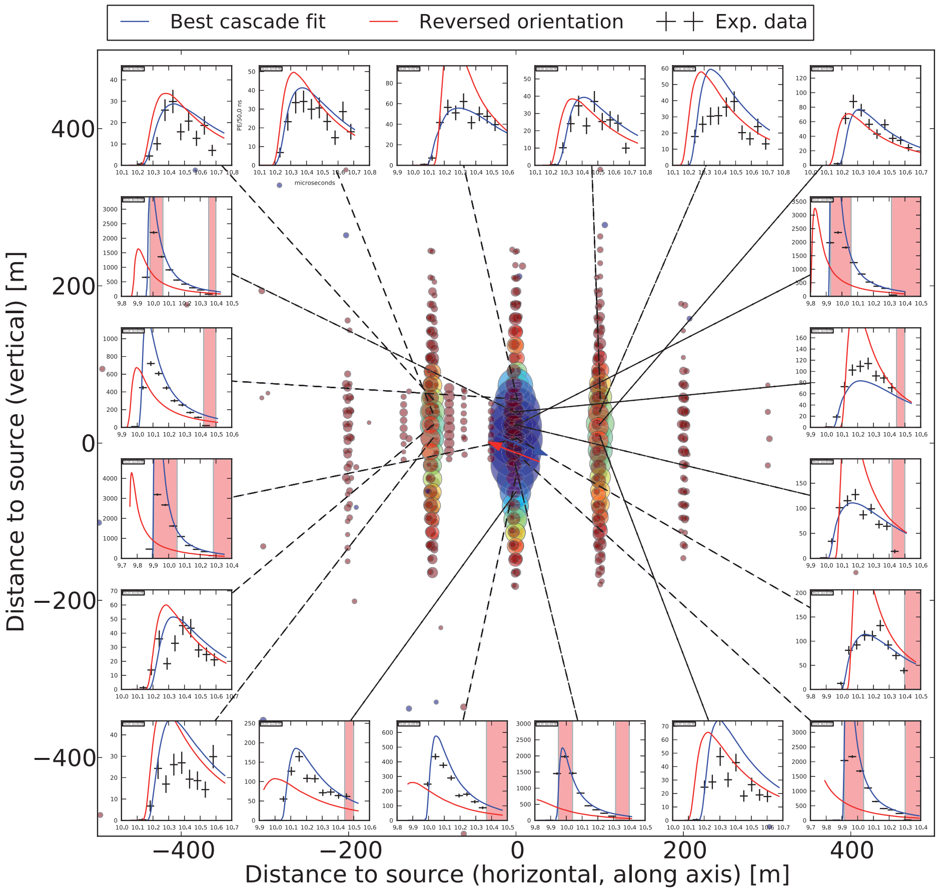

Fig. 10. – Representative signals captured by the DOM in one of the PeV events discussed in the text. The simulation reproduces the information collected by the DOM only when the correct energy and orientation are reached. While the 0.5 km size shower is nearly spherical, the waveforms positioned forward and backward relative to the direction of the incident neutrino are very different and reveal the neutrino direction. The neutrino moves horizontally from left to right.

6. – Sources of galactic cosmic rays

Despite the commissioning of instruments with improved sensitivity, it has been impossible to conclusively pinpoint Galactic PeVatrons by identifying gamma rays of pion origin. The position of the knee in the cosmic-ray spectrum indicates that some sources must accelerate cosmic rays to energies of several PeV. PeVatrons therefore produce pionic gamma rays whose spectrum extends to several hundred TeV without cutoff. In contrast, the widely studied supernova remnants RX J1713-3946 and RX J0852.0-4622 (Vela Junior) reach their maximum energy in the TeV region. In fact, recent data from Fermi LAT have directly challenged the hadronic interpretation of the GeV-TeV radiation from one of the best-studied candidates, RX J1713-3946 [50].

It is difficult to hide a Galactic cosmic accelerator from view. A generic supernova remnant releasing an energy W of about 10^{50} erg into the acceleration of cosmic rays will inevitably generate TeV gamma rays in the interaction of the accelerated cosmic rays with the hydrogen in the Galactic disk. The emissivity (number of particles produced per unit volume and time) in pionic gamma rays Q_γ is simply proportional to the density of cosmic rays $n_{\rm cr}$ and the density of the target $n \sim 1/{\rm cm}^3$ of cosmic rays in the disk. Here, $n_{\rm cr}$ $(> 1\,{\rm TeV}) \simeq 4 \times 10^{-14}\,{\rm cm}^{-3}$ is obtained by integrating the proton spectrum for energies in excess of 1 TeV. For an E^{-2} spectrum [51]

$$Q_\gamma \simeq c \left\langle \frac{E_\pi}{E_p} \right\rangle {\lambda_{pp}}^{-1}\, n_{\rm cr}\ (> 1\,{\rm TeV}) \simeq 2 c x_\gamma \sigma_{pp}\, n\, n_{\rm cr} \tag{18}$$

or

$$Q_\gamma\,(> 1\,{\rm TeV}) \simeq 10^{-29}\,{\rm cm}^{-3}\,{\rm s}^{-1} \left(\frac{n}{1\,{\rm cm}^{-3}}\right). \tag{19}$$

The proportionality factor in eq. (18) is determined by particle physics; $x_\gamma \simeq 0.1$ is the average energy of secondary photons relative to the cosmic-ray protons and $\lambda_{pp} = (n\sigma_{pp})^{-1}$ is the proton interaction length ($\sigma_{pp} \simeq 40\,{\rm mb}$) in a density n. The corresponding luminosity is

$$L_\gamma\,(>\ 1\,{\rm TeV}) \simeq Q_\gamma\, \frac{W}{\rho_E}\,, \tag{20}$$

where W/ρ_E is the volume occupied by the supernova remnant. Here we have made the approximation that the volume of the young remnant is given by W/ρ_E, or that the density of particles in the remnant is not very different from the ambient energy density $\rho_E \sim 10^{-12}\,{\rm erg\,cm}^{-3}$ of Galactic cosmic rays.

We thus predict [18] a rate of TeV photons from a supernova remnant at a nominal distance d on the order of 1 kpc of

$$\begin{aligned} \int_{E>1\,{\rm TeV}} \frac{{\rm d}N_\gamma}{{\rm d}E_\gamma} {\rm d}E_\gamma &= \int_{E>1\,{\rm TeV}} \frac{L_\gamma(>1\,{\rm TeV})}{4\pi d^2} {\rm d}E_\gamma \\ &\simeq 10^{-12}\text{–}10^{-11} \left(\frac{\rm photons}{{\rm cm}^2\,{\rm s}}\right)\left(\frac{W}{10^{50}\,{\rm erg}}\right)\left(\frac{n}{1\,{\rm cm}^{-3}}\right)\left(\frac{d}{1\,{\rm kpc}}\right)^{-2}. \end{aligned} \tag{21}$$

This is a PeVatron flux well within reach of the current generation of atmospheric gamma-ray telescopes; has it been detected?

Looking for them in the highest-energy survey of the Galactic plane points to the Milagro experiment [52]. Their survey in the $\sim 10\,{\rm TeV}$ band revealed a subset of sources located within nearby star-forming regions in Cygnus and in the vicinity of Galactic latitude $l = 40$ degrees. Subsequently, directional air Cherenkov telescopes were pointed at three of the sources [53, 54], revealing them as PeVatron candidates with gamma-ray fluxes in the range estimated above following an E^{-2} energy spectrum that extends to tens of TeV without evidence of a cutoff.

Interestingly, some of the sources cannot be readily associated with known supernova remnants, or with any non-thermal source observed at other wavelengths. These are

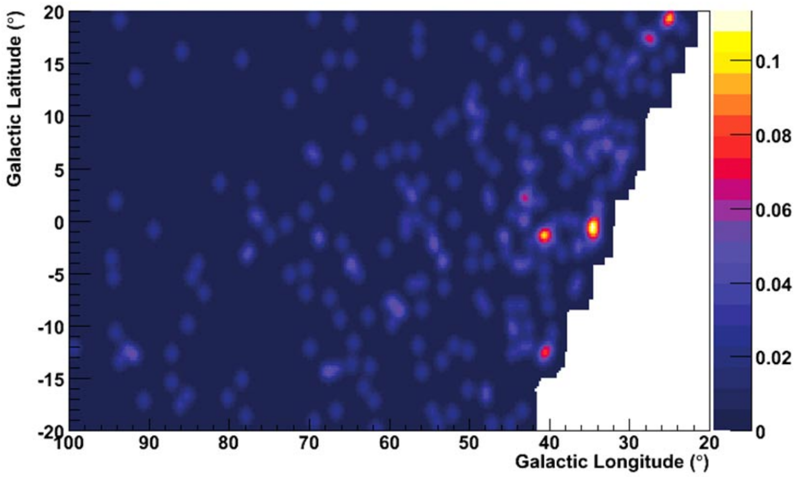

Fig. 11. – Simulated sky map of the probability distribution function [13] for point sources in Galactic coordinates after 5 years of operation of the completed IceCube detector. Two Milagro sources are visible with 4 events for MGRO J1852+01 and 3 events for MGRO J1908+06 with energy in excess of 40 TeV. These, as well as the background events, have been randomly distributed according to the resolution of the detector and the size of the sources.

likely to be molecular clouds illuminated by the cosmic-ray beam accelerated in young remnants located within about 100 pc. Indeed one expects that multi-PeV cosmic rays are accelerated only over a short time period when the shock velocity is high, *i.e.*, between free expansion and the beginning of its dissipation in the interstellar medium. The high-energy particles can produce photons and neutrinos over much longer periods when they diffuse through the interstellar medium to interact with nearby molecular clouds [55]. An association of molecular clouds and supernova remnants is expected in star-forming regions. In this case, any confusion of pionic with synchrotron photons is unlikely.

Assuming that the Milagro sources are indeed cosmic-ray accelerators, particle physics dictates the relation between pionic gamma rays and neutrinos and basically predicts the production of a $\nu_\mu + \bar{\nu}_\mu$ pair for every two gamma rays seen by Milagro. This calculation can be performed using the formalism introduced in the previous section with approximately the same outcome.

The quantitative statistics can be summarized as follows. For average values of the parameters in the flux expression, we find that the completed IceCube detector should confirm sources in the Milagro sky map as sites of cosmic-ray acceleration at the 3σ level in less than one year and at the 5σ level in three years [18]; see fig. 11. This assumes that the source extends to 300 TeV, or 10% of the energy of the cosmic rays near the knee in the spectrum. These results agree with previous estimates [56]. There are intrinsic ambiguities of an astrophysical nature in this estimate that may reduce or extend the time required for a 5σ observation [18]. Also, the extended nature of some of the Milagro sources represents a challenge for IceCube observations that are optimized for point sources. In the absence of an observation of TeV-energy supernova neutrinos by IceCube within a period of 10 years, the supernova origin of cosmic rays in the Galaxy will be challenged.

7. – Conclusion: stay tuned

In summary, IceCube was designed for a statistically significant detection of cosmic neutrinos accompanying cosmic rays in five years. Here we made the case that, based on multiwavelength information from ground-based gamma ray telescopes and cosmic-ray experiments, we are indeed closing in on supernova remnants, GRBs (if they are the sources of cosmic rays) and GZK neutrinos. The discussion brought to the forefront the critical role of improved spectral gamma-ray data on candidate cosmic-ray accelerators. The synergy between CTA [57], HAWC [58], IceCube, and KM3NeT as well as other next-generation neutrino detectors is likely to provide fertile ground for future progress.

* * *

This research was supported in part by the U.S. National Science Foundation under Grants No. OPP-0236449 and PHY-0969061; by the U.S. Department of Energy under Grant No. DE-FG02-95ER40896; by the University of Wisconsin Research Committee with funds granted by the Wisconsin Alumni Research Foundation.

REFERENCES

[1] Reines F. and Cowan C. L. Jr., *Nature*, **17** (1956) 446.
[2] Halzen F. and Klein S. R., *Phys. Today*, **61** N5 (2008) 29.
[3] Berezinsky V. S. and Zatsepin G. T., *Phys. Lett. B*, **28** (1969) 423.
[4] Roberts A., *Rev. Mod. Phys.*, **64** (1992) 259.
[5] Gaisser T. K., Halzen F. and Stanev T., *Phys. Rept.*, **258** (1995) 173 (Erratum **271** (1995) 355 (hep-ph/9410384)); Learned J. G. and Mannheim K., *Annu. Rev. Nucl. Part. Sci.*, **50** (2000) 679; Halzen F. and Hooper D., *Rep. Prog. Phys.*, **65** (2002) 1025 (astro-ph/0204527); Becker J., *Phys. Rept.*, **458** (2008) 173; Katz U. F. and Spiering C., *Prog. Part. Nucl. Phys.*, **67** (2012) 651 (astro-ph.HE/11110507).
[6] Markov M. A., in *Proceedings of the Tenth Annual International Conference on High Energy Physics at Rochester*, Vol. **578**, edited by Sudarshan E. C. G., Tinlot J. H. and Melissinos A. C. (University of Rochester, Rochester, NY) 1960, pp. 589-595.
[7] Babson J., Barish R., Becker-Szendy R. *et al.*, *Phys. Rev. D*, **42** (1990) 3613.
[8] Balkanov V. A. *et al.* (BAIKAL Collaboration), *Nucl. Phys. B Proc. Suppl.*, **118** (2003) 363.
[9] Aggouras G. *et al.* (NESTOR Collaboration), *Astropart. Phys.*, **23** (2005) 377.
[10] Aguilar J. A. *et al.* (ANTARES Collaboration), *Astropart. Phys.*, **26** (2006) 314.
[11] Migneco E., *J. Phys. Conf. Ser.*, **136** (2008) 022048.
[12] IceCube Collaboration, available at `http://www.icecube.wisc.edu/science/ publications/pdd/pdd.pdf` (2001).
[13] Ahrens J. *et al.* (IceCube Collaboration), *Astropart. Phys.*, **20** (2004) 507 (astro-ph/0305196).
[14] Becker J. K., *Phys. Rep.*, **458** (2008) 173 (astro-ph/07101557).
[15] Achterberg A. *et al.* (IceCube Collaboration), *Phys. Rev. D*, **76** (2007) 042008 *Erratum*, **77** (2007) 089904(E) (astro-ph/07051315).
[16] Ahlers M., Anchordoqui L. A., Gonzalez-Garcia M. C. *et al.*, *Astropart. Phys.*, **34** (2010) 106 (astro-ph.HE/10052620).
[17] Rhode W. *et al.* (Fréjus Collaboration), *Astropart Phys.*, **4** (1996) 217.
[18] Gonzalez-Garcia M. C., Halzen F. and Mohapatra S., *Astropart. Phys.*, **31** (2009) 437 (astro-ph.HE/09021176).
[19] Halzen F. and Saltzberg D., *Phys. Rev. Lett.*, **81** (1998) 4305 (arXiv:hep-ph/9804354).
[20] For a more detailed discussion of the analysis methods used by IceCube, see Halzen F., *Eur. Phys. J. C*, **46** (2006) 669 (astro-ph/0602132).

[21] Learned J. G. and Pakvasa S., *Astropart. Phys.*, **3** (1995) 267 (arXiv:hep-ph/9405296).
[22] Abbasi R. *et al.* (IceCube Collaboration), *Phys. Rev. D*, **86** (2012) 022005 (arXiv:1202.4564 [astro-ph.HE]).
[23] Spiering C., *AIP Conf. Proc.*, **1085** (2009) 18 (astro-ph/08114747).
[24] Katz U. and Spiering C., *Prog. Part. Nucl. Phys.*, **67** (2011) 651 (astro-ph.HE/11110507).
[25] Halzen F. and Klein S. R., *Rev. Sci. Instrum.*, **81** (2010) 081101 (astro-ph.HE/10071247).
[26] Woschnagg K. (AMANDA Collaboration), *Conf. Proc. C*, **990817V2** (1999) 200; updated optical properties are given in Chirkin D., in *Proc. XXXII ICRC, Beijing, China* (2011).
[27] Daum K. *et al.*, *Z. Phys. C*, **66** (1995) 417.
[28] Gonzalez-Garcia M. C., Maltoni M. and Rojo J., *High Energy Phys.*, **10** (2006) 75.
[29] Abbasi R. *et al.* (IceCube Collaboration), *Phys. Rev. D*, **79** (2009) 102005.
[30] Abbasi R. *et al.* (IceCube Collaboration), *Astropart. Phys.*, **34** (2010) 48.
[31] Abbasi R. *et al.* (IceCube Collaboration), *Phys. Rev. D*, **84** (2011) 082001.
[32] Abbasi R. *et al.* (IceCube Collaboration), *Phys. Rev. D*, **83** (2011) 012001.
[33] Barr G. D. *et al.*, *Phys. Rev. D*, **70** (2004) 023006.
[34] Enberg R., Reno M. H. and Sarcevic I., *Phys. Rev. D*, **78** (2008) 043005.
[35] Sommers P. and Westerhoff S., *New J. Phys.*, **11** (2009) 055004 (astro-ph/08021267); Hillas A. M., astro-ph/0607109v2 (2006); Berezinsky V., *J. Phys. Conf. Ser.*, **120** (2008) 012001 (astro-ph/08013028).
[36] Abbasi R. *et al.* (HiRes Collaboration), *Phys. Rev. Lett.*, **100** (2008) 101101 (astro-ph/0703099); Abraham J. *et al.* (Auger Collaboration), *Phys. Rev. Lett.*, **101** (2008) 061101 (astro-ph/08064302); Tokuno H. *et al.*, *J. Phys. Conf. Ser.*, **293** (2011) 012035.
[37] Baade W. and Zwicky F., *Proc. Natl. Acad. Sci. U.S.A.*, **20** (1934) 254.
[38] Butt Y., *Nature*, **460** (2009) 701 (astro-ph.he/10093664).
[39] Gaisser T. K., *OECD Megascience Forum, Taormina, Italy* (1997) (astro-ph/9707283) the discussion was revisited in Ahlers M., Anchordoqui L. A., Goldberg H. *et al.*, *Phys. Rev. D*, **72** (2005) 023001 (astro-ph/0503229).
[40] Waxman E., *Phys. Rev. Lett.*, **75** (1995) 386 (astro-ph/9701231) Vietri M., *Phys. Rev. Lett.*, **80** (1998) 3690 (astro-ph/9802241) and Bottcher M. and Dermer C. D., *Astrophys. J. Lett.*, **499** (1998) L131 (astro-ph/9801027v2).
[41] Waxman E. and Bahcall J., *Phys. Rev. D*, **59** (1998) 023002.
[42] Halzen F., *Acta Phys. Pol. B*, **42** (2011) 2525 (hep-ph/11111131).
[43] Ahlers M., Gonzalez-Garcia M. C. and Halzen F., *Astropart. Phys.*, **35** (2011) 87 (arXiv:1103.3421 [astro-ph.HE]).
[44] Abbasi R. *et al.* (IceCube Collaboration), *Nature*, **484** (2012) 351 (astro-ph.HE/1204.4219).
[45] Waxman E. and Bahcall J. N., *Phys. Rev. Lett.*, **78** (1997) 2292 (astro-ph/9701231).
[46] Alvarez-Muniz J. and Halzen F., *Astrophys. J.*, **576** (2002) L33 (astro-ph/0205408) for a more recent discussion of the formalism, see Becker J. K., Halzen F., O'Murchadha A. and Olivo M., *Astrophys. J.*, **721** (2010) 1891 (astro-ph.HE/09112202).
[47] Sullivan G., *Proceedings of Neutrino 2012, Kyoto, Japan*, to be published in *Nucl. Phys. B*.
[48] See ref. [14] above, and also Ackermann M. *et al.* (IceCube Collaboration), *Astrophys. J.*, **675** (2008) 1014 (astro.ph/07113022); Abbasi R. *et al.* (IceCube Collaboration), *Phys. Rev. D*, **82** (2010) 072003 (astro.ph.CO/10091442v1); Aynutdinov V. *et al.* (Baikal Collaboration), *Astropart. Phys.*, **25** (2006) 140 (astro-ph/0508675); Martens K. *et al.* (HiRes Collaboration), *Proceedings of 23rd Lepton-Photon Conference, Daegu, Korea (2007)* (astro-ph/07074417); Kravchenko I. *et al.* (RICE Collaboration), *Phys. Rev. D*, **73** (2006) 082002 (astro-ph/0601148); Barwick S. W. *et al.* (ANITA Collaboration), *Phys. Rev. Lett.*, **96** (2006) 171101 (astro-ph/0512265); Lehtinen N. G. *et al.*, *Phys. Rev. D*, **69** (2004) 013008 (astro-ph/0309656); Gorham P. W. *et al.*, *Phys. Rev. Lett.*, **93** (2004) 041101 (astro-ph/0310232); Anchordoqui L. A.

et al., *Phys. Rev. D*, **66** (2002) 103002 (hep-ph/0207139); Abbasi R. *et al.* (IceCube Collaboration), *Phys. Rev. D*, **84** (2011) 082001, also cited above.
[49] Ishihara A., *Proceedings of Neutrino 2012, Kyoto, Japan*, to be published in *Nucl. Phys. B*.
[50] Abdo A. A. *et al.* (Fermi-LAT Collaboration), *Astrophys. J.*, **734** (2011) 28 (astro-ph.HE/11035727v1).
[51] Berezinsky V. S., Gaisser T. K., Halzen F. and Stanev T., *Astropart. Phys.*, **1** (1993) 281.
[52] Abdo A. A. *et al.* (Milagro Collaboration), *Astrophys. J.*, **658** (2007) L33 (astro-ph/0611691).
[53] Djannati-Atai A. *et al.* (H.E.S.S. Collaboration), *30th ICRC, Merida, Mexico*, **OG2.2 2** (2007) 1316 (astro-ph/07102418).
[54] Albert J. *et al.*, *Astrophys. J.*, **675** (2008) L25 (astro-ph/0801.2391).
[55] Gabici S. and Aharonian F. A., *Astrophys. J.*, **665** (2008) 431 (astro-ph/07053011).
[56] Halzen F., Kappes A. and O'Murchadha A., *Phys. Rev. D*, **78** (2008) 063004, see also *Nucl. Instrum. Methods A*, **602** (2009) 117 (astro-ph/08030314v2).
[57] Cherenkov Telescope Array, `http://www.cta-observatory.org`.
[58] High-Altitude Water Cherenkov Observatory, `http://www.hawc.umd.edu`.